JCB Article

Differentiation- and stress-dependent nuclear cytoplasmic redistribution of myopodin, a novel actin-bundling protein

Astrid Weins,[1] Karin Schwarz,[1] Christian Faul,[1] Laura Barisoni,[2,3] Wolfgang A. Linke,[4] and Peter Mundel[1]

[1]Department of Medicine and Department of Anatomy and Cell Biology, Albert Einstein College of Medicine, Bronx, NY 10461
[2]Department of Pathology, Johns Hopkins University, Baltimore, MD 21287
[3]National Institute of Diabetes and Digestive and Kidney Diseases, National Institutes of Health, Bethesda, MD 20892
[4]Department of Physiology, University of Heidelberg, 69120 Heidelberg, Germany

We report the cloning and functional characterization of myopodin, the second member of the synaptopodin gene family. Myopodin shows no significant homology to any known protein except synaptopodin. Northern blot analysis resulted in a 3.6-kb transcript for mouse skeletal and heart muscle. Western blots showed an 80-kD signal for skeletal and a 95-kD signal for heart muscle. Myopodin contains one PPXY motif and multiple PXXP motifs. Myopodin colocalizes with α-actinin and is found at the Z-disc as shown by immunogold electron microscopy. In myoblasts, myopodin shows preferential nuclear localization. During myotube differentiation, myopodin binds to stress fibers in a punctuated pattern before incorporation into the Z-disc. Myopodin can directly bind to actin and contains a novel actin binding site in the center of the protein. Myopodin has actin-bundling activity as shown by formation of latrunculin-A–sensitive cytosolic actin bundles and nuclear actin loops in transfected cells expressing green fluorescent protein–myopodin. Under stress conditions, myopodin accumulates in the nucleus and is depleted from the cytoplasm. Nuclear export of myopodin is sensitive to leptomycin B, despite the absence of a classical nuclear export sequence. We propose a dual role for myopodin as a structural protein also participating in signaling pathways between the Z-disc and the nucleus.

Introduction

Vertebrate Z-discs are remarkably complex structures which serve several important functions: (a) they stably anchor actin filaments during contraction, a requirement for the transmission of mechanical strain along the serially linked sarcomeres and ultimately, along the length of the muscle. (b) They provide a point of attachment for other cytoskeletal proteins, such as desmin, nebulin, and titin. In particular, the giant sarcomeric titin filaments, which are mainly responsible for the elasticity and passive tension development of relaxed muscles, are in need of such anchorage because strain is also transmitted across the Z-disc in the nonactivated, stretched muscle fiber. (c) To efficiently transmit the strain, it appears that the Z-discs of both skeletal and cardiac muscle respond dynamically to mechanical stress through transitions in their lattice structure (Goldstein et al., 1986, 1989).

Although the Z-disc is generally viewed as the site where actin filaments from opposing half-sarcomeres are cross-linked by α-actinin, it has become clear over the past years that more proteins are involved in the formation of the common structural unit of all Z-discs, the Z-unit. Most notably, the NH_2 terminus of titin participates by providing binding sites for α-actinin (Ohtsuka et al., 1997; Sorimachi et al., 1997; Young et al., 1998) and T-cap/telethonin (for review see Gregorio et al., 1999). Further, nebulin (and nebulette in cardiac muscle; Moncman and Wang, 1995) also enters the Z-disc at its COOH terminus (Labeit and Kolmerer, 1995; Millevoi et al., 1998), it is possible that this polypeptide also provides attachment sites for α-actinin, actin, and perhaps titin. At the periphery of the Z-disc, interaction between actin and titin has been reported in cardiac muscle, thereby rendering this titin region functionally inextensible (Linke et al., 1997; Trombitas and Granzier, 1997). However, the peripheral Z-disc region of titin could well be complexed with

Address correspondence to Peter Mundel, Division of Nephrology, Albert Einstein College of Medicine, 1300 Morris Park Ave., Bronx, NY 10461. Tel.: (718) 430-3219. Fax: (718) 430-8963.
E-mail: mundel@aecom.yu.edu

Astrid Weins and Karin Schwarz contributed equally to this paper.

Key words: actin-binding protein; muscle differentiation; nuclear-cytoplasmic translocation; synaptopodin gene family; Z-disc

F-actin by additional proteins. A potential candidate to form ternary complexes with actin and titin is myopodin, the second member of the synaptopodin gene family.

Synaptopodin is a proline-rich actin-associated protein, strongly expressed in differentiated kidney glomerular podocytes and telencephalic dendrites. Due to its high content of equally distributed proline residues, synaptopodin is a linear molecule without globular domains. In both brain and kidney, the gene expression is differentiation dependent (Mundel et al., 1997a). This is consistent with data obtained from cultured podocytes, in which synaptopodin expression occurs during differentiation and coincides with growth arrest and process formation (Mundel et al., 1997b). Database searches with the synaptopodin cDNA identified an expressed sequence tag (EST)* clone from human skeletal muscle that showed ~50% homology in a region of 95 amino acids. Here, we describe the corresponding protein, which we termed myopodin. Evidence is provided that myopodin has actin-binding and -bundling activity and shuttles between the nucleus and the cytoplasm in a differentiation-dependent and stress-induced fashion. We also discuss the possible role of myopodin in the nucleus.

Results

Myopodin is a novel member of the synaptopodin gene family

From a human skeletal muscle library screen, 38 independent clones were obtained in two rounds of screening. These clones were partially overlapping and covered the ORF of human myopodin (Fig. 1). From a mouse skeletal muscle library screening, we obtained 13 independent clones, all of which started upstream of the ATG and contained several stop codons before the ATG. From a mouse heart library, 20 independent clones were isolated. Out of these, 8 clones started upstream of the ATG and contained several stop codons before the ATG. Of note, no sequence differences were found between mouse skeletal muscle and heart (Fig. 1). Molecular cloning of mouse myopodin revealed an ORF of 2,274 bp and an additional 1,481 bp 3′-untranslated region. The ORF codes for a 757 amino acid (aa) protein with a calculated M_r of 80.9 kD and an isoelectric point of 9.35. At the protein level, an identity of 87.5% was found between human and mouse myopodin. The overall homology between myopodin and synaptopodin was 47.7%, with the highest degree of homology residing in the COOH-terminal half of the molecules (Fig. 1).

Based on sequence comparisons using the BLASTP and BLASTN algorithms (Altschul et al., 1990), myopodin showed no significant homology to other published proteins except synaptopodin (Mundel et al., 1997a) and genethonin 2 (AF177291), which represents a 132 amino acid fragment of myopodin. Similar to synaptopodin, due to its high content of proline residues (~13%) which are evenly distributed along the protein, myopodin may not form globular domains. Several potential phosphorylation sites are present throughout the

Figure 1. **Sequence alignment of human and mouse synaptopodin and myopodin.** Deduced amino acid sequence (one letter code) of human and mouse synaptopodin cDNA (top lanes) and myopodin (bottom lanes). At the protein level, an overall identity of 46% is found between both proteins. Synaptopodin contains two PPXY motifs (bold), myopodin contains only one PPXY motif. Multiple PXXP motifs are found throughout both molecules. Myopodin contains two potential NLSs (bold and underlined) not found in synaptopodin. Synaptopodin, but not myopodin, contains two possible PEST sites (underlined in italics) between aa 44 and 88 (PEST score: 11.72) and between aa 327 and 342 (PEST score: 6.17). The sequence data of myopodin are available from GenBank/EMBL/DDBJ under accession nos. AJ010482 (human) and AJ306625 (mouse). Myopodin peptides used for immunization are bold and boxed (SRIB1) or boxed (SRIB2).

*Abbreviations used in this paper: aa, amino acid; EST, expressed sequence tag; GFP, green fluorescent protein; lat-A, latrunculin A; LMB, leptomycin B; NES, nuclear export sequence; NLS, nuclear localization signal; NS, nuclear shuttling.

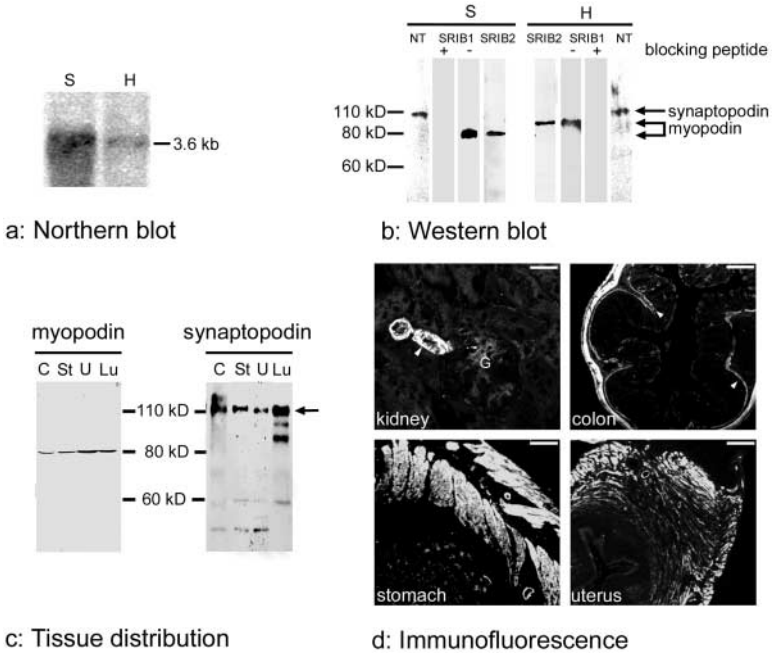

Figure 2. **Expression of myopodin in skeletal, heart, and smooth muscle cells.** (a) A single 3.6 kB mRNA is detected in mouse skeletal muscle (S) and heart (H). The expression in the heart is weaker than in skeletal muscle. (b) Western blot analysis of myopodin and synaptopodin in cytosolic extracts of mouse skeletal (S) and heart (H) muscle. A 110-kD band corresponding to synaptopodin is found in both tissues using antisynaptopodin antibody NT. The myopodin antibody SRIB1 reveals a band of 80-kD in skeletal muscle and ~95 kD in the heart (Fig. 2 b). Both signals were blocked with the corresponding peptide showing the specificity of the bands. Identical results were obtained for SRIB2 (Fig. 2 b). (c) Western blot analysis of myopodin (left) in colon (C), stomach (St), uterus (U), and lung (Lu) shows a single 80-kD band in all lanes. Interestingly the same tissues also express synaptopodin (right, arrow). (d) Immunofluorescence microscopy of myopodin in mouse kidney, colon, stomach, and uterus. In the kidney, myopodin is strongly expressed in arteriolar smooth muscle cells (arrowhead), but not in glomerular (G) podocytes. In colon, stomach, and uterus myopodin expression is restricted to smooth muscle cells. In the colon, the arrowheads mark the muscularis mucosae. Bars: (kidney) 40 μm; (stomach, colon, and uterus) 300 μm.

molecule. Although synaptopodin contains two PPXY motifs (Mundel et al., 1997a), myopodin contains only one PPXY motif, which is preserved between human and mouse (Fig. 1). PPXY motifs mediate protein–protein interactions between proline-rich peptide stretches and protein interaction modules, such as WW domains (Kay et al., 2000). Several PXXP motifs are found throughout the molecule, which represent potential binding sites for SH3 domain–containing proteins. Myopodin contains two potential classical nuclear localization signals (NLSs) (Hicks and Raikhel, 1995), one in the NH_2-terminal region and one in the COOH-terminal region of the molecule, both of which are preserved between human and mouse (Fig. 1). In contrast, no NLS are present in synaptopodin. We did not observe a classical nuclear export sequence (NES) in myopodin. Using the PESTfind program for the prediction of potential PEST regions, which target proteins for rapid degradation (Rechsteiner and Rogers, 1996), we detected two high score PEST sites in synaptopodin but not in myopodin (Fig. 1).

A single 3.6-kb myopodin mRNA encodes an 80-kD protein in skeletal muscle and a 95-kD protein in the heart

Northern blots were performed with 400 ng of polyA$^+$ RNA from mouse skeletal and heart muscle. A strong band of ~3.6 kD was detected in skeletal muscle and in the heart a somewhat weaker expression of the same band was seen (Fig. 2 a). Immunoblots of cytosolic extracts from mouse skeletal and heart muscle with antimyopodin antibody SRIB1 showed one band of 80 kD in skeletal muscle and one band of 95 kD in the heart, corresponding to myopodin (Fig. 2 b). The expression was stronger in skeletal muscle than in the heart. Since Northern blot analysis revealed only one message for both skeletal muscle and heart tissues (Fig. 2 a) the different molecular weight on protein level seems to be due to posttranslational modification. Similar findings have been described previously for synaptopodin (Mundel et al., 1997a). Preincubation with the SRIB1 peptide used for immunization blocked the immunoreaction, thereby showing the specificity of the myopodin bands (Fig. 2 b). Identical results were obtained with the myopodin-specific SRIB2 antibody (Fig. 2 b and unpublished data). Using the synaptopodin antibody NT, a major band of 110 kD was found in both tissues, which was clearly different from the myopodin band seen with SRIB1 and SRIB2. Similar to synaptopodin (Mundel et al., 1997a), myopodin is highly susceptible to proteolytic degradation. Several proteolytic myopodin fragments could be detected by Western blot analysis when extracts from muscle tissues where stored at −20°C instead of direct boiling in SDS sample buffer (unpublished data).

Myopodin is widely expressed in striated and smooth muscle cells

The tissue distribution of myopodin was analyzed by Western blot and immunochemistry. By Western blot with the myopodin-specific antibody SRIB2, an 80-kD band was detected in colon, stomach, uterus, and lung (Fig. 2 c, left). A weak band of 80 kD was found in glomerular preparations after prolonged exposure (60 min; unpublished data). The glomerular band was presumably due to contaminating cells from adjacent glomerular arterioles rather than intraglomerular expression. No myopodin immunostaining could be detected in glomeruli, but a strong signal was found in smooth muscle cells of glomerular arterioles (Fig. 2 d). In stomach, colon, and uterus, myopodin expression was restricted to muscle cell layers as shown by immunofluorescence microscopy (Fig. 2 d).

Myopodin localizes to the Z-disc in mature striated muscle

To determine the intracellular distribution of myopodin, frozen tissue sections from skeletal and heart muscle were immu-

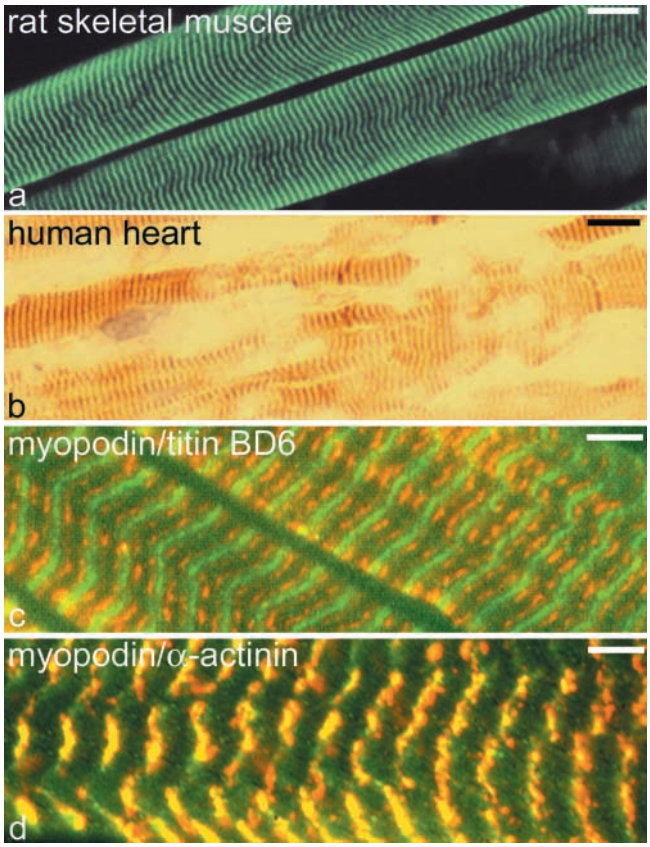

Figure 3. **Immunohistochemistry of myopodin in skeletal and heart muscle.** (a) Immunofluorescence labeling of a rat skeletal muscle frozen section with antimyopodin SRIB1 shows a striated pattern. (b) In the human heart, a similar striated pattern is seen. (c and d) Double labeling of rat skeletal muscle with titin (c) and α-actinin (d). Myopodin is shown in green, titin and α-actinin in red. (c) Antititin BD6 localizes to the A-I junction and encircles the myopodin labeling. (d) Myopodin colocalizes with α-actinin at the Z-disk. The overlap of immunoreactivity results in a yellow staining of the Z-disks (d).

nostained with SRIB1 and SRIB2. A striated pattern was observed in skeletal (Fig. 3 a) and heart muscle (Fig. 3 b). The localization of myopodin in the sarcomere was further analyzed in double labeling experiments with antibodies against titin (Fig. 3 c) and α-actinin (Fig. 3 d). The epitope stained by the titin antibody BD6, which localizes to the A–I junction (Whiting et al., 1989), flanked the myopodin epitope but did not overlap with it (Fig. 3 c). In contrast, α-actinin, which is a constituent of the Z-disc, completely overlapped with myopodin (Fig. 3 d), indicating that myopodin is localized in the Z-disc region. Preabsorption of both antisera with the corresponding peptides abrogated the immunolabeling, thereby proving the specificity of the Z-line staining (unpublished data). The association of myopodin with the Z-disc was confirmed by immunogold labeling. On ultra-thin frozen sections from stretched rat psoas muscle and heart, the electron-dense gold particles, representing sites of myopodin expression, were found at the center (Fig. 4 a) and periphery of the Z-disc (Fig. 4 b), but were absent from other parts of the sarcomere (Fig. 4 a). In the heart, myopodin was also detected at the Z-disc (Fig. 4 c). This staining pattern was comparable to that found for α-actinin, an established component of the Z-disc (unpublished data).

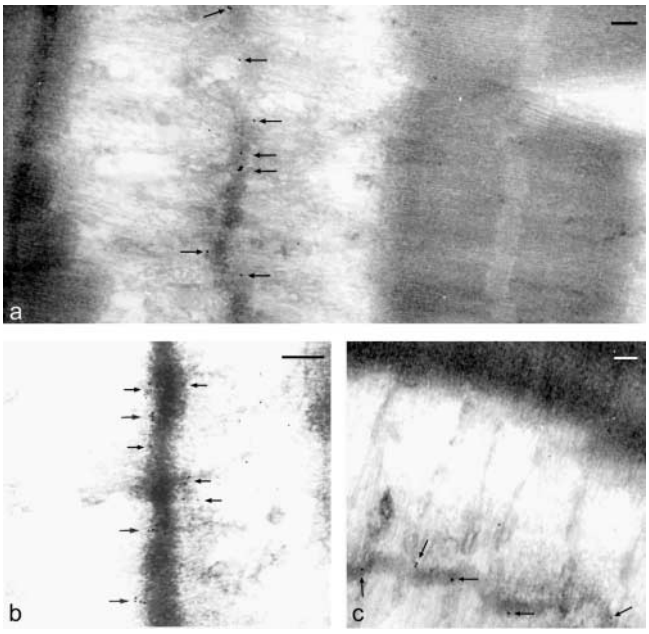

Figure 4. **Immunoelectron microscopic analysis of myopodin.** Immunoelectron microscopy of ultrathin frozen sections from stretched rat psoas muscle (a and b) and rat heart (c). The arrows point to the localization of myopodin at the Z-disc of skeletal and heart muscle. Bars, 0.4 μm.

Differentiation-dependent nuclear cytoplasmic redistribution of myopodin in C2C12 cells

Next, the expression of myopodin was analyzed by immunofluorescence microscopy in C2C12 cells, which serve as a well-characterized in vitro model system of skeletal muscle differentiation (Yaffe and Saxel, 1977; Blau et al., 1985). In undifferentiated myoblasts, myopodin was strongly expressed in the nucleus, leaving the nucleoli free, and very weakly in the cytoplasm (Fig. 5 a). After as little as 6 h after induction of myotube differentiation, myopodin was clearly found in both the nucleus and the cytoplasm along actin filaments (Fig. 5 b). During the progression of myotube differentiation, myopodin was found in a dotted pattern along the actin filaments (Fig. 5 c). In differentiated myotubes, myopodin was found at the Z-disc in a pattern comparable to the expression in vivo (Fig. 5 d; see Fig. 3 for comparison), but it was no longer observed in the nucleus (Fig. 5 d). Northern blot analysis detected a 3.6-kB band of comparable intensity in myoblasts and myotubes (Fig. 5 e). In contrast, at the protein level a clear upregulation of myopodin was found in myotubes. These findings show a differentiation-dependent intracellular redistribution and a posttranscriptional regulation of myopodin expression.

Myopodin directly binds to actin

Since myopodin was found along actin fibers in myoblasts (Fig. 5, b and c), we tested whether myopodin directly binds to actin. To this end, spin-down assays with purified chicken actin and in vitro translated ^{35}S-labeled myopodin were performed (Fig. 6 a). As expected for an actin-binding protein, most of the radio-labeled myopodin (~65% of labeled protein) was found in the 100,000 *g* pellet (Fig. 6 a,

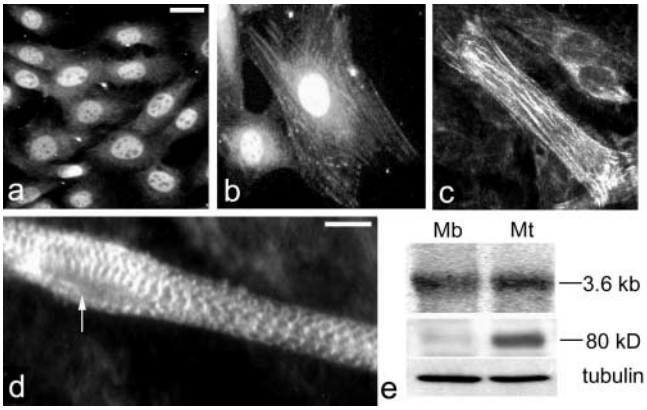

Figure 5. **Differentiation-dependent nuclear cytoplasmic redistribution of myopodin in C2C12 cells.** C2C12 cells were analyzed by immunofluorescence microscopy at different time points of differentiation using SRIB2 antibody. (a) In proliferating myoblasts, myopodin was strongly expressed in the nucleus, but only weakly in the cytoplasm. (b) Soon (6 h) after induction of myocyte differentiation, myopodin was found in the nucleus and in the cytoplasm along actin filaments. (c) Later myopodin was seen in a dotted pattern along the actin filaments. (d) In differentiated myotubes, it was found at the Z-disc in a pattern resembling that found in adult muscle fibers (compare with Fig. 3 a), and was no longer in the nucleus (arrow). (e) Northern blot analysis (top lanes) detected a 3.6-kB transcript in myoblasts (Mb) and myotubes (Mt). Western blot analysis (middle) revealed a strong up-regulation of protein expression in Mt. Equal protein loading was confirmed by reprobing with α-tubulin (bottom). Bars: (a) 40 μm; (d) 20 μm.

left). Furthermore, labeled protein was excluded from the pellet by adding increasing amounts of unlabeled myopodin as a competitor (Fig. 6 a, right). In the presence of a threefold excess of cold myopodin, >70% of radio-labeled protein remained in the 100,000 *g* supernatant (Fig. 6 a), thus confirming the specificity of the myopodin–actin interaction. No difference in the actin binding capacity was detected when G-actin was allowed to polymerize before the addition of myopodin (unpublished data).

Myopodin contains a novel actin-binding site between aa 410 and 563

Myopodin binds to actin (Fig. 6, a and b), but no classical actin-binding site is present in the protein. Therefore, the actin-binding site was determined by a green fluorescent protein (GFP) truncation approach. A series of cDNA fragments of variable length were generated that overlapped with each other and covered the complete ORF of myopodin. These fragments were cloned into the pEGFP-C1 expression vector, transfected into C2C12 myoblasts growing in differentiation medium, and analyzed by direct fluorescence microscopy in living cells. A minimal fragment spanning aa 410 and 563 (termed MP7) was sufficient and necessary for the association with actin filaments (Fig. 7). Further truncation of this fragment resulted in the loss of the actin-binding ability (Fig. 7).

Overexpression of myopodin-GFP reveals latrunculin-A–sensitive actin-bundling activity in A7 cells and myoblasts

To start unraveling the possible function of myopodin, A7 cells (Cunningham et al., 1992) and C2C12 myoblasts growing in differentiation medium were transiently transfected with full-length myopodin as an EGFP fusion protein. Then, cells were analyzed by colabeling with DAPI as a nuclear marker and rhodamine-conjugated phalloidin to stain actin fibers. Myopodin expression induced massive actin bundles in the cytosol (Fig. 8, a and b, arrows) and actin-containing loops in the nucleus (Fig. 8, a and b, arrowheads). In ~80% of transfected, currently differentiating, C2C12 cells, GFP-myopodin was found along the stress fibers in a punctuated pattern and was also detected in a striated pattern in differentiated myotubes, indicating Z-disc localization (unpublished data). In the remaining ~20% of the transfected cells, all of which were undifferentiated myoblasts, giant intranuclear myopodin containing loops formed (Fig. 8 c). These loops were readily visible by phase contrast microscopy and were similar in appearance to the nuclear loops induced by supervillin (Wulfkuhle et al., 1999). Like the supervillin-induced nuclear loops the myopodin-induced loops contained actin as revealed by double labeling with rhodamine-conjugated phalloidin (Fig. 8 c), but not α-actinin or titin (unpublished data). In contrast to the supervillin-induced loops, the myopodin-induced loops did not colocalize with lamin (unpublished data) and were sensitive to treatment with latrunculin A (lat-A). 2 h after treatment with lat-A, the myopodin-GFP loops had disassembled and showed a diffuse intranuclear redistribution (Fig. 8 d). This disassembly was fully reversible. After washout of lat-A, the loops reappeared and after 4 h they were completely restored (Fig. 8 d, arrows). Hence, myopodin has actin bundling activity, but the dynamics of the myopodin-induced nuclear loops are different from those of the supervillin-induced loops. In contrast, transfection studies with synaptopodin-GFP constructs

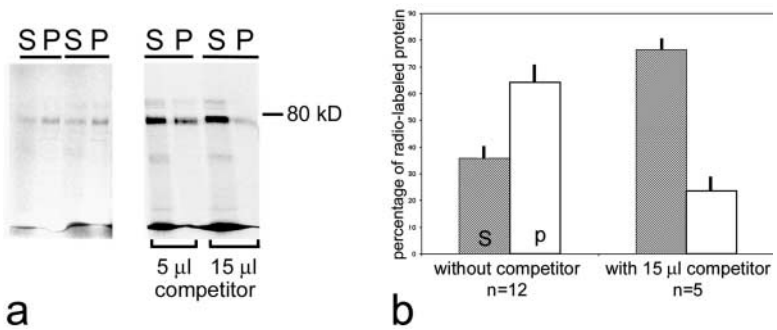

Figure 6. **Myopodin directly binds to actin.** (a) Detection of radio-labeled myopodin by actin cosedimentation in the 100,00 *g* pellet (P; left). In the presence of cold myopodin as a competitor (right), most of the labeled protein remains in the supernatant (S). (b) Densitometric quantification reveals that >65% of radio-labeled myopodin is found in the pellet (P). In the presence of unlabeled myopodin as competitor, >70% of radioactive-labeled protein remains in the supernatant (S).

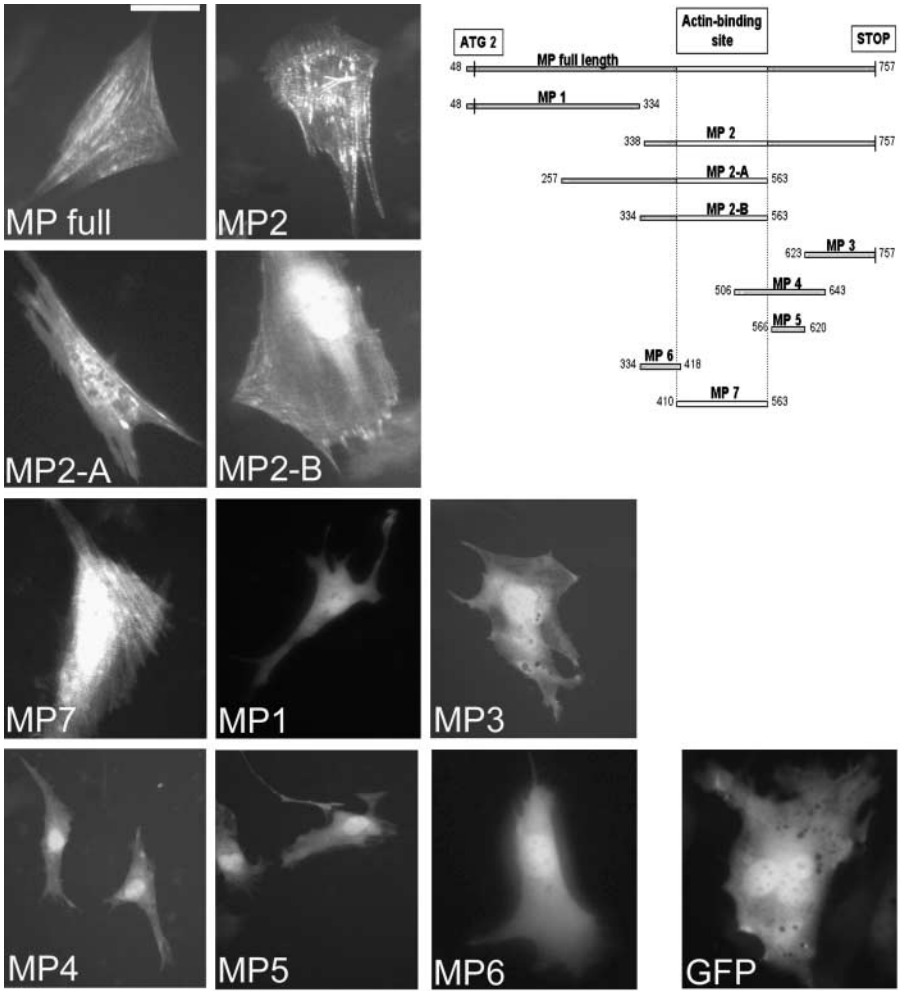

Figure 7. **Myopodin contains a novel actin binding site.** C2C12 myoblasts were transfected with myopodin-GFP constructs of variable length. In addition to full-length myopodin (MP full), constructs were generated which contained various fragments of the ORF. With this approach, a single actin binding site of myopodin was defined that corresponds to fragment MP7. pEGFP-C1 alone did not bind to the actin filaments. Bar, 30 μm.

showed actin binding and bundling in the cytoplasm, but not in the nucleus (unpublished data).

The mutation of two potential NLSs does not affect the nuclear translocation of myopodin

Myopodin contains two potential consensus NLSs (NH_2-terminal:KKRR and COOH-terminal:KKGK(K); Figs. 1 and 9 a) which may target the protein to the nucleus. Indeed, myopodin is found in the nucleus of undifferentiated C2C12 myoblasts (Fig. 5 a). Therefore, we tested whether the nuclear import of myopodin was mediated by one or both putative NLSs present. First, we showed that in the absence of the NH_2-terminal NLS1, the fragment MP2 still translocated into the nucleus (unpublished data). To test the possibility that the nuclear import of myopodin was mediated by the COOH-terminal NLS, site-directed mutagenesis was used to generate two GFP full-length constructs, one in which only the COOH-terminal NLS was mutated (termed mut 2) and another in which both NLSs were mutated (termed mut 1+2). Both mut 2 and mut1+2 were still able to translocate into the nucleus and induce nuclear-acting bundling (Fig. 9 b). Based on these results, we conclude that neither NLS is required for the nuclear import of myopodin in myoblasts, although we cannot rule out the possibility that the NLSs may be operative under different conditions.

Stress-induced nuclear accumulation of myopodin in myoblasts and myotubes

Many NLSs containing proteins continuously shuttle between the cytoplasm and the nucleus, whereas other proteins are found in the nucleus only under certain conditions (Mattaj and Englmeier, 1998). The actin-binding protein cofilin is normally present in the cytoplasm, but after treatment of myogenic cells with DMSO, the cells form intranuclear rod structures that contain actin and cofilin (Ono et al., 1993). The intranuclear actin rods also develop after heat shock of cultured mammalian cells (Iida et al., 1986). To test whether myopodin was redistributed under stress, C2C12 myoblasts were heat shocked at 43°C (Iida et al., 1986). In ~80% of the heat-shocked cells, the induction of actin- and myopodin-containing nuclear rods (arrows) was observed by double immunofluorescence microcopy after 150 min (Fig. 10, a–c). Many of the rod-containing cells showed a disrupted actin cytoskeleton as revealed by the absence of stress fibers in the cytoplasm. Similar changes could be observed already after 90 min of heat shock, although the effect was less severe (unpublished data). We also tested whether the inhibition of CRM1-dependent nuclear export by leptomycin B (LMB) (Nishi et al., 1994) in combination with a 90 min heat shock caused a nuclear accumulation and cytoplasmic depletion of myopodin. Therefore, 10 nM LMB was added to the culture

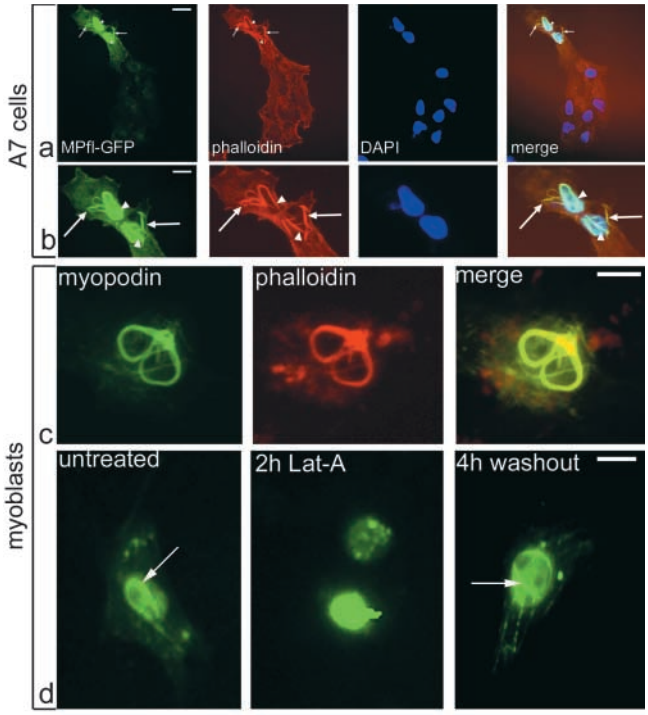

Figure 8. **Overexpression of myopodin reveals actin bundling activity.** (a) Immunofluorescence of A7 cells transfected with a myopodin full-length GFP (MPfl-GFP). Actin fibers are labeled with rhodamine-conjugated phalloidin and nuclei are stained with DAPI. Expression of myopodin induces actin bundles in the cytoplasm (arrows) and actin loops in the nucleus (arrowheads). Note the absence of actin bundles in nontransfected cells. (b) High power view of transfected cells seen in panel a. In the triple-labeling (merge), intranuclear actin loops appear blue-white (arrowheads) and cytosolic actin bundles yellow (arrows). (c) C2C12 myoblasts transfected with GFP-myopodin develop giant nuclear loops. Myopodin-induced loops contain actin as revealed by double labeling with rhodamine-conjugated phalloidin, but not α-actinin or titin (unpublished data). (d) Myopodin-induced actin loops (arrows) are sensitive to lat-A. Bars: (a) 80 μm; (b) 30 μm; (c and d) 10 μm.

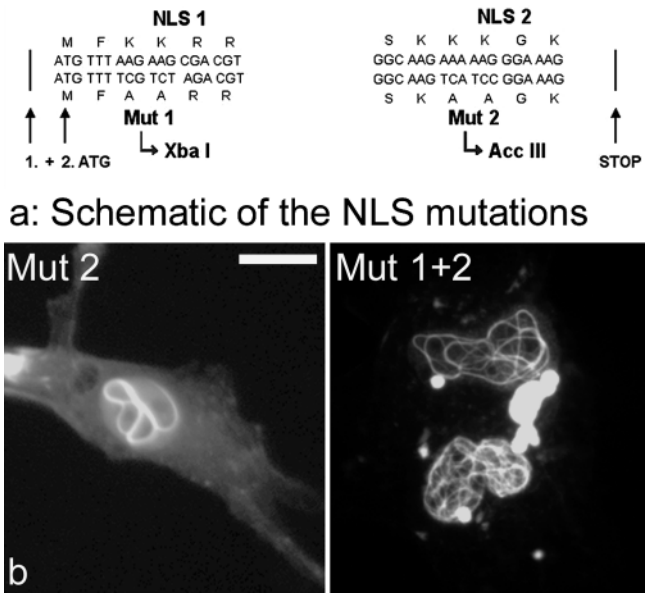

Figure 9. **The two potential NLSs are not required for nuclear import of myopodin.** (a) Inactivation of two potential NLSs present in myopodin by site directed mutagenesis. (b) Myopodin is transported to the nucleus and induces nuclear actin bundling after inactivation of the COOH-terminal NLS (mut 2) alone or after inactivation of both the COOH-terminal NLS and the NH_2-terminal NLS (mut 1+2). Bar, 20 μm.

medium 5 min before the heat shock. In all cells a clear effect was noted: myopodin was depleted from the cytoplasm and accumulated in the nucleus (Fig. 10 e), often in a fine, speckled pattern (Fig. 10 f). Finally, to test whether myopodin can shuttle into the nucleus even after incorporation into a mature Z-disk, heat shock experiments were performed with differentiated myotubes. Under these conditions, myopodin was depleted from the Z-disc and accumulated in the nucleus (Fig. 10, g–i). These data show that myopodin shuttles between the nucleus and the cytoplasm in myoblasts and myotubes and that nuclear export of myopodin occurs in a CRM1-dependent fashion.

Discussion

In the present study, we describe the cloning and functional characterization of the actin-binding protein myopodin, a novel member of the synaptopodin gene family (Mundel et al., 1997a). Myopodin and synaptopodin share a high degree of homology at the primary sequence level as well as some fundamental structural and functional properties. On the other hand, they also show significant differences that may allow them to exert different functions in the cell.

As described previously for synaptopodin (Mundel et al., 1997a), myopodin seems to be differentially modified in different tissues. Northern blot analysis revealed only one message of ~3.6 kb in both heart and skeletal muscle (Fig. 2 a). However, by Western blot analysis, a protein of ~80 kD was detected in skeletal muscle, whereas the corresponding protein in the heart had a size of ~95 kD (Fig. 2 b). The cause of this size difference remains to be established, but for several reasons, it appears to be due to posttranslational modification(s). First, cDNA sequencing of mouse skeletal muscle and heart myopodin revealed identical results. Second, the same message could be detected in both heart and skeletal muscle (Fig. 2 a). Third, alternative splicing can be ruled out because myopodin is an intronless gene (unpublished data). Fourth, in vitro translation from the myopodin cDNA gives only one product of ~80 kD (Fig. 6 a). Finally, both polyclonal antisera (SRIB1 and SRIB2) directed against different internal peptides revealed the same results on Western blots (Fig. 2 b).

The high degree of overall homology of ~50% with synaptopodin gave the first hint of the function of myopodin. Both proteins are rich in prolines (synaptopodin 20%, myopodin 13%), which are equally distributed along the molecule and may result in a linear protein structure and may explain the high susceptibility to proteolytic degradation of both proteins. Myopodin and synaptopodin are rapidly degraded in protein extracts stored at −20°C before dilution with SDS sample buffer and boiling (unpublished data). On the other hand, this degradation could be avoided when protein extracts were directly mixed with SDS sample buffer

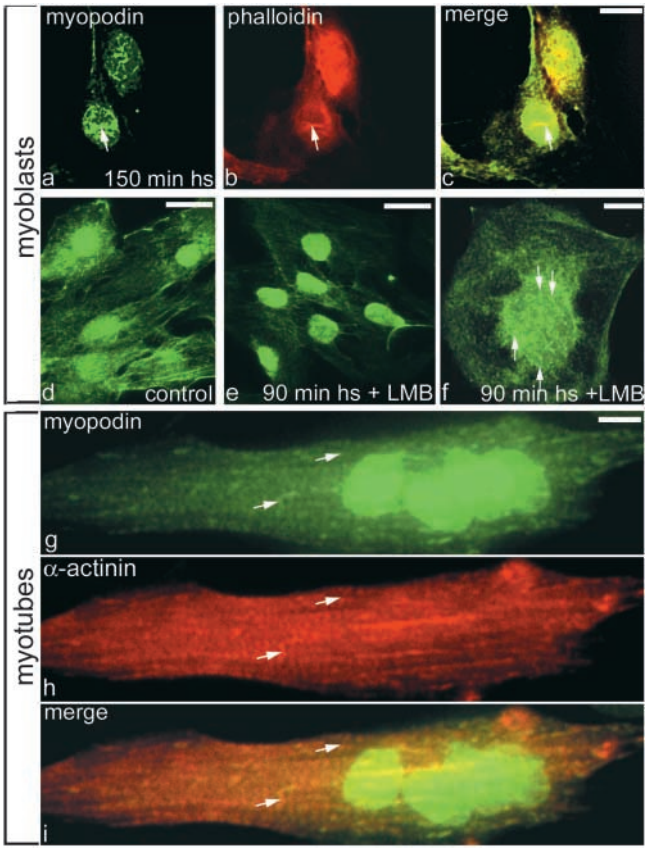

Figure 10. **Stress-induced nuclear actin rod formation and redistribution of myopodin.** (a–c) Formation of myopodin (a) and actin (b) containing intranuclear rods (arrows) in myoblasts after a 150 min heat shock. (d–f) Nuclear accumulation and cytoplasmic depletion of myopodin after 90 min heat shock in the presence of 10 μm LMB (e). (f) In some cells, a punctuated pattern of nuclear myopodin redistribution was noted. (g–i) After heat shock of differentiated myotubes, myopodin (g) shuttles from the Z-disk (arrows; see Fig. 5 d for control) visualized by α-actinin staining (h) to the nucleus. Bars: (a–e) 40 μm; (f–i) 20 μm.

and boiled. In fact, synaptopodin, but not myopodin, contains two so-called PEST motifs (Fig. 1) that may target the protein to rapid degradation by the proteasome (Rechsteiner and Rogers, 1996). A linear structure would also allow fast and efficient interactions with multiple other proteins. The idea of myopodin serving as an adaptor protein is supported by the presence of multiple PXXP motifs for potential SH3 domain binding and by the presence of a single PPXY motif in myopodin, which is conserved between mouse and human (Fig. 1). PPXY motifs mediate the interaction with the WW domain of a variety of structural and signal transduction proteins (Kay et al., 2000). In contrast to synaptopodin, myopodin contains two potential NLS (see below).

Myopodin (Fig. 6, a and b) and synaptopodin (unpublished data) directly bind to actin. In skeletal and heart muscle, myopodin (Fig. 4) and synaptopodin (unpublished data) are found at the Z-disc. In fibroblasts, α-actinin and the stress fiber proteins have an arrangement similar to that in striated muscle. Based on these observations, a sarcomeric model of stress fiber structure in nonmuscle cells was proposed (Sanger et al., 1983). The regular and punctuated arrangement of synaptopodin along the actin filaments in podocytes (Mundel et al., 1997a,b), the colocalization of myopodin and synaptopodin with α-actinin in differentiating myoblasts and transfected NIH3T3 cells (unpublished data) indicate that members of the synaptopodin gene family may be involved in the organization or regulation of the Z-disc in striated muscle cells and a Z-disc equivalent in podocytes.

The expression of synaptopodin in neurons and podocytes is restricted to late stages of cellular differentiation (Mundel et al., 1997a). In podocytes, synaptopodin expression coincides with process formation and reorganization of the actin cytoskeleton and is a marker of a differentiated podocyte phenotype (Mundel et al., 1991). During myocyte differentiation, synaptopodin is constitutively expressed in both undifferentiated myoblasts and differentiated myotubes without changes in protein expression levels (unpublished data). In contrast, myopodin is regulated in a temporal and spatial fashion during myocyte differentiation (Fig. 5). In undifferentiated myoblasts, myopodin is expressed preferentially in the nucleus and only weakly in the cytoplasm. In differentiated myotubes it is incorporated into the Z-disc and shows no detectable nuclear expression (Fig. 5, c and d). Notably, this redistribution coincides with an increase in protein expression (Fig. 5 e). Together, these findings indicate that myopodin may be involved in the regulation of myocyte differentiation, a function not shared with synaptopodin.

The most significant difference between myopodin and synaptopodin is the ability of myopodin to translocate into the nucleus and induce nuclear actin bundling. We noted thick bundles of filamentous actin in the nuclei of cells overexpressing GFP-myopodin (Fig. 8), but never in nuclei of cells expressing GFP-synaptopodin (unpublished data). The loops were similar in appearance to those induced by supervillin (Wulfkuhle et al., 1999). Supervillin is a membrane-associated, F-actin–binding protein of the villin/gelsolin superfamily (Pestonjamasp et al., 1997). Similar to myopodin, supervillin contains several NLSs, translocates to the nucleus, and bundles F-actin (Wulfkuhle et al., 1999). However, in contrast to the supervillin-induced loops, the myopodin-induced loops are sensitive to disruption of actin filaments with lat-A (Fig. 8) and do not contain the nuclear cytoskeleton protein lamin (unpublished data). The functional significance of the nuclear actin loops remains elusive. They may simply represent an artifact of strong overexpression. On the other hand, they show the actin-bundling activity of myopodin and its ability to translocate into the nucleus.

It remains to be established whether the myopodin-induced actin bundles arise from a pool of preexisting nuclear actin alone or whether their formation requires additional import of cytoplasmic actin. There is growing evidence for both constitutive presence in and import of actin and actin-associated proteins into the nucleus. The COOH-terminal domain of lamin A binds to nuclear actin, suggesting that an actin-associating molecular motor linked to the nuclear lamina could be involved in the movement or modification of chromatin domains (Sasseville and Langelier, 1998). This hypothesis is further supported by the finding that type I myosin is present in the nucleus (Nowak et al., 1997). A novel isoform of nonmuscle α-actinin, termed actinin-4, shifted steadily from the cytoplasm to the nucleus upon in-

hibition of phosphatidylinositol 3 kinase or actin depolymerization (Honda et al., 1998). Conformational differences between cytoplasmic and nuclear actin were described using a monoclonal antibody (Gonsior et al., 1999). This antibody, 2G2, recognizes a specific conformation of native actin which is present in the nucleus and specified by compaction of the antibody-reactive region into a coherent patch (Gonsior et al., 1999). Actin itself contains two NES sequences in the middle part of the molecule, and LMB treatment of cells prevented nuclear exclusion of endogenous actin, inducing its nuclear accumulation (Wada et al., 1998). Expression of actin mutants with disrupted NESs, but not of wild-type actin, induced a decrease in the proliferative potential of the cell, indicating a role of actin in cell division (Wada et al., 1998). Zyxin, a regulator of actin filaments, shuttles between focal contacts and the nucleus (Nix and Beckerle, 1997), where it targets the mitotic apparatus by interacting with the h-warts/LATS1 tumor suppressor (Hirota et al., 2000). The EAST protein of *Drosophila* controls an expandable nuclear endoskeleton by promoting nuclear import of CP60 and actin (Wasser and Chia, 2000). Together, these findings indicate that components of the actin cytoskeleton are present in the nucleus under physiological conditions. Modulation of nuclear actin content or polymerization state may be required to maintain normal cell function. Further studies will aim to define the precise role of myopodin in these processes.

In addition to a role under physiological conditions, there is growing evidence for a role of the actin cytoskeleton in the nucleus in situations of cellular stress. Sanger et al. (1980) showed a reversible translocation of cytoplasmic actin into the nucleus and formation of intranuclear actin filament bundles after treatment with DMSO. Subsequently, Ono et al. (1993) showed the association of cofilin with nuclear actin and proposed that nuclear import of actin in DMSO-treated cells is mediated by cofilin. Similar results were obtained in heat-shocked cells (Courgeon et al., 1993). Interestingly, T cell costimulation causes nuclear translocation of cofilin (Samstag et al., 1994) and inhibition of the translocation by dephosphorylation induces T cell apoptosis (Samstag et al., 1996). We now show that heat shock of myoblasts (Fig. 10, a–f) and myotubes (Fig. 10, g–i) induces cytoplasmic depletion and nuclear accumulation of myopodin, even after incorporation into a mature Z-disc. This nuclear accumulation was even stronger after inhibition of CRM1-mediated nuclear export with LMB. As described above, actin has two NESs and accumulates in the nucleus after inactivation of the NESs (Wada et al., 1998). In contrast, myopodin does not have a known NES (Fig. 1), but still accumulates in the nucleus after LBM treatment (Fig. 10). Therefore, future studies will have to clarify whether the nuclear accumulation of myopodin is mediated by a novel NES or via binding to actin or another NES-carrying protein. In any case, our studies indicate a role of myopodin in situations of cellular stress. The stress might trigger certain cellular responses during which myopodin may serve as a signaling or regulator molecule.

Another intriguing question is how myopodin is translocated into the nucleus. The two potential NLSs present in the molecule appear to be not necessary for nuclear import, since deletion or inactivation by mutagenesis of both NLSs did not prevent nuclear import and actin bundling in myoblasts (Fig. 9, a and b). In addition to NLS-mediated nuclear import, proteins can be imported into the nucleus through so-called nuclear-shuttling (NS) sequences (Michael, 2000). NS sequences are stretches of 30 and 60 aa and bind to transportin proteins that mediate both nuclear import and export (Michael, 2000). All proteins currently known to contain this type of signal also associate with mRNA. In contrast to basic amino acid type NLSs and leucine-rich NESs, the NS motifs are less well preserved and therefore need to be experimentally established for each protein (Michael, 2000). Future studies will focus on testing whether myopodin contains a (novel) NS or whether it shuttles between the cytoplasm by binding to another protein, including actin.

What could be the functional role of myopodin? Myopodin directly binds to actin. It bundles actin filaments, both in the cytoplasm and in the nucleus, and is found along cytoplasmic actin filaments in a punctuated pattern and at the Z-disc, where it colocalizes with α-actinin. In contrast, in the nucleus myopodin is not coexpressed with α-actinin, indicating that myopodin may interact with different proteins in the cytoplasm and the nucleus. In the nucleus, myopodin shows a speckled pattern reminiscent of actin snRNP aggregates (Sahlas et al., 1993). Thus, one can imagine that myopodin is involved in an actin-based mRNA transport pathway. Alternatively, it may bundle nuclear actin and thereby modulate the actin-based nuclear endoskeleton similar to the *Drosophila* EAST protein (Wasser and Chia, 2000). Striated muscle cells are highly differentiated and specialized cells that must be able to adequately respond to various physiological and pathological challenges. We propose that, similar to zyxin at focal contacts (Nix and Beckerle, 1997), myopodin may play a dual role as a structural protein at the Z-disc and a regulator protein participating in a signaling pathway between the nucleus and the Z-disc during development and in situations of cellular stress.

Materials and methods

cDNA cloning and sequencing

Database searches with the cDNA sequence of synaptopodin identified one EST clone (EMBL/GenBank/DDBJ accession no. AA100598; Research Genetics). Human skeletal muscle myopodin was cloned by cDNA library screening and RACE-PCR (CLONTECH Laboratories, Inc.). The mouse homologue of myopodin was cloned by cDNA library screening from mouse skeletal muscle and heart cDNA libraries. Sequence alignments, analyses, and database searches were done with the NIH BLAST algorithms (www.ncbi.nlm.nih.gov/BLAST) (Altschul et al., 1990).

RNA isolation and Northern blot analysis

Total RNA was isolated from mouse skeletal and heart muscle with the RNeasy Kit (QIAGEN) according to the manufacturer's instructions. PolyA$^+$ mRNA was purified with the Oligotex mRNA Purification Kit (QIAGEN), separated on a 1.2% denaturing formaldehyde gel, and transferred onto GeneScreen Plus membranes (NEN Life Science Products). Northern blot analyses were done with a ^{32}P-labeled antisense riboprobe using a 1750-bp fragment of the mouse heart cDNA as template.

Site-directed mutagenesis

The two potential NLSs were inactivated using the Quikchange site-directed mutagenesis kit (Stratagene) by replacing the first two arginines in each NLS with two alanines (Fig. 9 a). Diagnostics digests at newly arising cutting sites and subsequent DNA sequencing confirmed the effective mutagenesis. We generated two GFP full-length constructs, one in which only the COOH-terminal NLS was mutated (mut2) and one in which both NLS were mutated (mut 1+2).

Antibodies

Two polyclonal antisera specific for myopodin were generated by immunization of rabbits with a keyhole limpet hemocyanin-conjugated peptides. The antisera were affinity purified as described previously for synaptopodin (Mundel et al., 1997a). Antisera SRIB1 was directed against aa 634–652 (single letter code SGRGAQLFAKRQSRMEKYV, bold and boxed in Fig. 1), and SRIB2 directed against aa 593–612 (single letter code FKGPQAAVASQNYTPKPTVS, boxed in Fig. 1) of human myopodin. Antisynaptopodin polyclonal antiserum NT has been described previously (Mundel et al., 1997a).

Immunochemistry

Adult female rats were perfused via the abdominal aorta with 4% PFA in PBS for 3 min at 220 mm Hg followed by cryoprotectant sucrose PBS solution (800 mOsmol) for 5 min at 220 mm Hg. Organs were harvested and tissue slices were frozen in liquid isopentane (Mundel et al., 1997a). 5-μm thick frozen sections from rat heart and skeletal muscle were incubated with SRIB1 (1:25) and SRIB2 (1:10) and NT (1:50). Double labelings were done with monoclonal antibody BD6 against titin (Whiting et al., 1989) and sarcomeric α-actinin (Sigma-Aldrich). Immunofluorescence labeling and documentation were done as described previously (Mundel et al., 1997a). The specificity of the myopodin reaction was verified by preabsorption with the corresponding peptides that had been used for immunization. For human heart, 3-μm thick serial sections of formalin-fixed paraffin-embedded tissue were rehydrated in a graded series of alcohol and stained using an avidin-biotin immunoperoxidase technique (Barisoni et al., 1999).

Immunoelectron microscopy

Psoas muscle stretched to different degrees in situ was excised from freshly killed rats, which had been previously perfused with PBS containing 4% paraformaldehyde. Cryosectioning and immunogold labeling with SRIB1 and SRIB2 as well as anti–α-actinin (Sigma-Aldrich) followed by 10-nm gold particle–conjugated secondary antibodies was essentially as described (Mundel et al., 1991; Linke et al., 1998).

Protein extraction and immunoblotting

Skeletal muscles and hearts were harvested from adult C67 black mice. Protein extraction was performed at 4°C in a tight-fitting Potter homogenizer with 15 strokes at 1,400 rpm in 10 vol of homogenization buffer (20 mM Tris, 500 mM NaCl, pH 7.5) supplemented with 1% Triton X-100 (Sigma-Aldrich), 5 mM EDTA, and the following protease inhibitors (all from Roche Diagnostics): 2 μM pepstatin, 2 μM leupeptin, and 200 μM pefabloc. Insoluble material was pelleted at 50,000 *g* for 35 min at 4°C. The resulting supernatants were immediately diluted with SDS sample buffer, boiled for 5 min, and separated on 8% SDS polyacrylamide gels to avoid proteolysis of myopodin. Proteins were transferred to Immobilon P membranes (Millipore) by semidry blotting. SRIB1 and SRIB2 were used at 1:250, NT was used at 1:1:200, HRP-conjugated secondary antibodies (Promega) at 1:20,000. The immunoreaction was visualized by ECL (Amersham Pharmacia Biotech) and film exposure. The specificity of the myopodin reaction was verified by preabsorption with the corresponding peptide used for immunization. To explore the expression of myopodin in organs other than skeletal and heart muscle, cytosolic extracts from colon, stomach, uterus, lung, brain and liver were analyzed by immunoblotting. In addition, proteins were extracted from C2C12 myoblasts and myotubes.

Cell culture

C2C12 myoblasts (Yaffe and Saxel, 1977; Blau et al., 1985) were propagated in DME with 4 mM L-glutamine, 1 mM sodium pyruvate and 1.5 g/l sodium bicarbonate, supplemented with 10% FBS. Differentiation was induced by replacing FBS with 2% horse serum when the cells reached 80% confluence. For immunostaining, myoblasts were plated on collagen-coated coverslips. 6 d after switching to horse serum, cells were fixed and processed for immunocytochemistry. M2 cells (ABP280/filamin-deficient) and A7 cells (ABP280/filamin-repleted M2 cells) (Cunningham et al., 1992) were cultured in MEM containing 8% newborn calf serum and 2% fetal calf serum. In case of the rescued A7 cells, G418 (500 μg/ml) was added to retain expression of ABP280/filamin.

Actin cosedimentation

In vitro translation of full-length myopodin was done with the TnT coupled reticulocyte lysate kit (Promega) in the presence of 1 μg plasmid DNA and either ^{35}S-labeled methionine (Amersham Pharmacia Biotech) or unlabeled amino acid mix. Actin cosedimentation assays were essentially performed as described previously (Kaplan et al., 2000). For competitive binding assays, 5 or 15 μl of unlabeled in vitro–translated myopodin was added to the cosedimentation mix. Myopodin bands were quantified with ImageQuant Software and expressed as a percentage of total labeled protein found in supernatant and pellet (Kaplan et al., 2000).

Mapping of the actin binding site

Myopodin cDNA constructs of decreasing length covering the complete ORF (see Fig. 7) were cloned into the pEGFP-C1 expression vector (CLONTECH). The constructs were transfected into subconfluent myoblasts using GenePORTER transfection reagent (Gene Therapy Systems) and analyzed by direct fluorescence microscopy in living cells. Pictures were captured with a Spot cooled CCD camera (Diagnostic Instruments) and processed with Adobe Photoshop® 5.0 software.

Reversible disruption of the actin cytoskeleton with lat-A

2 d after transfection with GFP-myopodin, cells were treated with 5 μM lat-A (Calbiochem) for 2 h to depolymerize actin filaments (Coue et al., 1987). The effects of lat-A were observed in living cells as described in the previous section. The cells were washed twice with PBS and further cultivated for 4 h in the absence of lat-A to show reversibility.

Heat shock and LMB treatment

C2C12 myoblast and myotubes were incubated for 90–150 min at 43°C in a waterbath. In some experiments 10 nM LMB (Sigma-Aldrich) was added to the medium 5 min before heat shock induction to block nuclear export (Nishi et al., 1994). After heat shock, cells were fixed and processed for immunocytochemistry.

We thank Torsten Heider and Hiltraud Hosser for expert technical assistance. The monoclonal antibody BD6 against titin was provided by Dr. John Trinick (University of Leeds, Leeds, UK). M2 cells and A7 cells were a gift of Dr. T. Stossel (Brigham and Women's Hospital, Boston, MA). We would also like to thank Drs. Hanh T. Ngyen, Jeffrey E. Segall, U. Thomas Meier, and John S. Condeelis, AECOM, for critical reading of the manuscript.

Wolfgang A. Linke is a Heisenberg fellow of the German Research Foundation. This work was supported by a grant from the Howard Hughes Medical Research Institute Research Resources for Medical Schools and the National Institutes of Health (DK57683-01) to Peter Mundel.

Submitted: 11 December 2000
Revised: 31 August 2001
Accepted: 26 September 2001

References

Altschul, S.F., W. Gish, W. Miller, E.W. Myers, and D.J. Lipman. 1990. Basic local alignment search tool. *J. Mol. Biol.* 215:403–410.

Barisoni, L., W. Kriz, P. Mundel, and V. D'Agati. 1999. The dysregulated podocyte phenotype: a novel concept in the pathogenesis of collapsing idiopathic focal segmental glomerulosclerosis and HIV-associated nephropathy. *J. Am. Soc. Nephrol.* 10:51–61.

Blau, H.M., G.K. Pavlath, E.C. Hardeman, C.P. Chiu, L. Silberstein, S.G. Webster, S.C. Miller, and C. Webster. 1985. Plasticity of the differentiated state. *Science.* 230:758–766.

Coue, M., S.L. Brenner, I. Spector, and E.D. Korn. 1987. Inhibition of actin polymerization by latrunculin A. *FEBS Lett.* 213:316–318.

Courgeon, A.M., M. Maingourd, C. Maisonhaute, C. Montmory, E. Rollet, R.M. Tanguay, and M. Best-Belpomme. 1993. Effect of hydrogen peroxide on cytoskeletal proteins of *Drosophila* cells: comparison with heat shock and other stresses. *Exp. Cell Res.* 204:30–37.

Cunningham, C.C., J.B. Gorlin, D.J. Kwiatkowski, J.H. Hartwig, P.A. Janmey, H.R. Byers, and T.P. Stossel. 1992. Actin-binding protein requirement for cortical stability and efficient locomotion. *Science.* 255:325–327.

Goldstein, M.A., L.H. Michael, J.P. Schroeter, and R.L. Sass. 1986. The Z-band lattice in skeletal muscle before, during and after tetanic contraction. *J. Muscle Res. Cell Motil.* 7:527–536.

Goldstein, M.A., L.H. Michael, J.P. Schroeter, and R.L. Sass. 1989. Two structural states of Z-bands in cardiac muscle. *Am. J. Physiol.* 256:H552–H559.

Gonsior, S.M., S. Platz, S. Buchmeier, U. Scheer, B.M. Jockusch, and H. Hinssen. 1999. Conformational difference between nuclear and cytoplasmic actin as detected by a monoclonal antibody. *J. Cell Sci.* 112:797–809.

Gregorio, C.C., H. Granzier, H. Sorimachi, and S. Labeit. 1999. Muscle assembly: a titanic achievement? *Curr. Opin. Cell Biol.* 11:18–25.

Hicks, G.R., and N.V. Raikhel. 1995. Protein import into the nucleus: an integrated view. *Annu. Rev. Cell Dev. Biol.* 11:155–188.

Hirota, T., T. Morisaki, Y. Nishiyama, T. Marumoto, K. Tada, T. Hara, N. Masuko, M. Inagaki, K. Hatakeyama, and H. Saya. 2000. Zyxin, a regulator of actin filament assembly, targets the mitotic apparatus by interacting with h-warts/LATS1 tumor suppressor. *J. Cell Biol.* 149:1073–1086.

Honda, K., T. Yamada, R. Endo, Y. Ino, M. Gotoh, H. Tsuda, Y. Yamada, H. Chiba, and S. Hirohashi. 1998. Actinin-4, a novel actin-bundling protein associated with cell motility and cancer invasion. *J. Cell Biol.* 140:1383–1393 (erratum published 143:277).

Iida, K., H. Iida, and I. Yahara. 1986. Heat shock induction of intranuclear actin rods in cultured mammalian cells. *Exp. Cell Res.* 165:207–215.

Kaplan, J.M., S.H. Kim, K.N. North, H. Rennke, L.A. Correia, H.Q. Tong, B.J. Mathis, J.C. Rodriguez-Perez, P.G. Allen, A.H. Beggs, and M.R. Pollak. 2000. Mutations in ACTN4, encoding α-actinin-4, cause familial focal segmental glomerulosclerosis. *Nat. Genet.* 24:251–256.

Kay, B.K., M.P. Williamson, and M. Sudol. 2000. The importance of being proline: the interaction of proline-rich motifs in signaling proteins with their cognate domains. *FASEB J.* 14:231–241.

Labeit, S., and B. Kolmerer. 1995. The complete primary structure of human nebulin and its correlation to muscle structure. *J. Mol. Biol.* 248:308–315.

Linke, W.A., M. Ivemeyer, P. Mundel, M.R. Stockmeier, and B. Kolmerer. 1998. Nature of PEVK-titin elasticity in skeletal muscle. *Proc. Natl. Acad. Sci. USA.* 95:8052–8057.

Linke, W.A., M. Ivemeyer, S. Labeit, H. Hinssen, J.C. Ruegg, and M. Gautel. 1997. Actin-titin interaction in cardiac myofibrils: probing a physiological role. *Biophys. J.* 73:905–919.

Mattaj, I.W., and L. Englmeier. 1998. Nucleocytoplasmic transport: the soluble phase. *Annu. Rev. Biochem.* 67:265–306.

Michael, W.M. 2000. Nucleocytoplasmic shuttling signals: two for the price of one. *Trends Cell Biol.* 10:46–50.

Millevoi, S., K. Trombitas, B. Kolmerer, S. Kostin, J. Schaper, K. Pelin, H. Granzier, and S. Labeit. 1998. Characterization of nebulette and nebulin and emerging concepts of their roles for vertebrate Z-discs. *J. Mol. Biol.* 282: 111–123.

Moncman, C.L., and K. Wang. 1995. Nebulette: a 107 kD nebulin-like protein in cardiac muscle. *Cell Motil. Cytoskeleton.* 32:205–225.

Mundel, P., P. Gilbert, and W. Kriz. 1991. Podocytes in glomerulus of rat kidney express a characteristic 44 KD protein. *J. Histochem. Cytochem.* 39:1047–1056.

Mundel, P., H.W. Heid, T.M. Mundel, M. Kruger, J. Reiser, and W. Kriz. 1997a. Synaptopodin: an actin-associated protein in telencephalic dendrites and renal podocytes. *J. Cell Biol.* 139:193–204.

Mundel, P., J. Reiser, A.Z. Borja, H. Pavenstadt, G.R. Davidson, W. Kriz, and R. Zeller. 1997b. Rearrangements of the cytoskeleton and cell contacts induce process formation during differentiation of conditionally immortalized mouse podocyte cell lines. *Exp. Cell Res.* 236:248–258.

Nishi, K., M. Yoshida, D. Fujiwara, M. Nishikawa, S. Horinouchi, and T. Beppu. 1994. Leptomycin B targets a regulatory cascade of crm1, a fission yeast nuclear protein, involved in control of higher order chromosome structure and gene expression. *J. Biol. Chem.* 269:6320–6324.

Nix, D.A., and M.C. Beckerle. 1997. Nuclear-cytoplasmic shuttling of the focal contact protein, zyxin: a potential mechanism for communication between sites of cell adhesion and the nucleus. *J. Cell Biol.* 138:1139–1147.

Nowak, G., L. Pestic-Dragovich, P. Hozak, A. Philimonenko, C. Simerly, G. Schatten, and P. de Lanerolle. 1997. Evidence for the presence of myosin I in the nucleus. *J. Biol. Chem.* 272:17176–17181.

Ohtsuka, H., H. Yajima, K. Maruyama, and S. Kimura. 1997. Binding of the N-terminal 63 kDa portion of connectin/titin to α-actinin as revealed by the yeast two hybrid system. *FEBS Letters.* 401:65–67.

Ono, S., H. Abe, R. Nagaoka, and T. Obinata. 1993. Colocalization of ADF and cofilin in intranuclear actin rods of cultured muscle cells. *J. Muscle Res. Cell Motil.* 14:195–204.

Pestonjamasp, K.N., R.K. Pope, J.D. Wulfkuhle, and E.J. Luna. 1997. Supervillin (p205): a novel membrane-associated, F-actin-binding protein in the villin/gelsolin superfamily. *J. Cell Biol.* 139:1255–1269.

Rechsteiner, M., and S.W. Rogers. 1996. PEST sequences and regulation by proteolysis. *Trends Biochem Sci.* 21:267–271.

Sahlas, D.J., K. Milankov, P.C. Park, and U. De Boni. 1993. Distribution of snRNPs, splicing factor SC-35 and actin in interphase nuclei: immunocytochemical evidence for differential distribution during changes in functional states. *J. Cell Sci.* 105:347–357.

Samstag, Y., E.M. Dreizler, A. Ambach, G. Sczakiel, and S.C. Meuer. 1996. Inhibition of constitutive serine phosphatase activity in T lymphoma cells results in phosphorylation of pp19/cofilin and induces apoptosis. *J. Immunol.* 156: 4167–4173.

Samstag, Y., C. Eckerskorn, S. Wesselborg, S. Henning, R. Wallich, and S.C. Meuer. 1994. Costimulatory signals for human T-cell activation induce nuclear translocation of pp19/cofilin. *Proc. Natl. Acad. Sci. USA.* 91:4494–4498.

Sanger, J.W., J.M. Sanger, and B.M. Jockusch. 1983. Differences in the stress fibers between fibroblasts and epithelial cells. *J. Cell Biol.* 96:961–969.

Sanger, J.W., J.M. Sanger, T.E. Kreis, and B.M. Jockusch. 1980. Reversible translocation of cytoplasmic actin into the nucleus caused by dimethyl sulfoxide. *Proc. Natl. Acad. Sci. USA.* 77:5268–5272.

Sasseville, A.M., and Y. Langelier. 1998. In vitro interaction of the carboxy-terminal domain of lamin A with actin. *FEBS Lett.* 425:485–489.

Sorimachi, H., A. Freiburg, B. Kolmerer, S. Ishiura, G. Stier, C.C. Gregorio, D. Labeit, W.A. Linke, K. Suzuki, and S. Labeit. 1997. Tissue-specific expression and α-actinin binding properties of the Z-disc titin: implications for the nature of vertebrate Z-discs. *J. Mol. Biol.* 1997:688–695.

Trombitas, K., and H. Granzier. 1997. Actin removal from cardiac myocytes shows that near Z line titin attaches to actin while under tension. *Am. J. Physiol.* 273:C662–C670.

Wada, A., M. Fukuda, M. Mishima, and E. Nishida. 1998. Nuclear export of actin: a novel mechanism regulating the subcellular localization of a major cytoskeletal protein. *EMBO J.* 17:1635–1641.

Wasser, M., and W. Chia. 2000. The EAST protein of *Drosophila* controls an expandable nuclear endoskeleton. *Nat. Cell Biol.* 2:268–275.

Whiting, A., J. Wardale, and J. Trinick. 1989. Does titin regulate the length of muscle thick filaments? *J. Mol. Biol.* 205:263–268.

Wulfkuhle, J.D., I.E. Donina, N.H. Stark, R.K. Pope, K.N. Pestonjamasp, M.L. Niswonger, and E.J. Luna. 1999. Domain analysis of supervillin, an F-actin bundling plasma membrane protein with functional nuclear localization signals. *J. Cell Sci.* 112:2125–2136.

Yaffe, D., and O. Saxel. 1977. Serial passaging and differentiation of myogenic cells isolated from dystrophic mouse muscle. *Nature.* 270:725–727.

Young, P., C. Ferguson, S. Banuelos, and M. Gautel. 1998. Molecular structure of the sarcomeric Z-disk: two types of titin interactions lead to an asymmetrical sorting of alpha-actinin. *EMBO J.* 17:1614–1624.